Structural Engineering and Mechanics, Vol. 44, No. 2 (2012) 163-178

DOI: http://dx.doi.org/10.12989/sem.2012.44.2.163

Modeling of non-seismically detailed columns subjected to reversed cyclic loadings

Cao Thanh Ngoc Tran*

Department of Civil Engineering, International University, Vietnam National University, Ho Chi Minh City, Vietnam

(Received April 11, 2012, Revised August 27, 2012, Accepted September 26, 2012)

Abstract. A strut-and-tie model is introduced in this paper to predict the ultimate shear strength of non-seismically detailed columns. The validity and applicability of the proposed strut-and-tie model are evaluated by comparison with available experimental data. The model was developed based on visible crack patterns observed on the test specimens. The concrete contribution is integrated into the strut-and-tie model through a concept of equivalent transverse reinforcement. To further validate the model a full-scale non-seismically detailed reinforced concrete column was tested to investigate its seismic behavior. The specimen was tested under the combination of a constant axial load, $0.30f_c'A_g$ and quasi-static cyclic loadings simulating earthquake actions. Quasi-static cyclic loadings simulating earthquake actions were applied to the specimen until it could not sustain the applied axial load. The analytical results reveal that the strut-and-tie method is capable of modeling to a satisfactory accuracy the ultimate shear strength of non-seismically detailed columns subjected to reserved cyclic loadings.

Keywords: reinforced concrete columns; strut-and-tie; seismic; shear strength

1. Introduction

The strut-and-tie analogy (Khoo 2007, Yang 2011, Brown 2006, Zhang 2007, Kiousis 2010) is the discrete modeling of actual stress fields in the reinforced concrete member. The complex stress fields inside the structural members resulting from applied external forces are simplified into discrete compressive and tensile force paths. The general idea of this analogy is to use concrete to carry compressive forces and steel reinforcement to carry tensile forces. The longitudinal reinforcement in a member represents the tensile chord of a truss while the concrete in the flexural compression zone can be considered as part of the longitudinal compressive chord. The transverse reinforcement serves as transverse ties joining the longitudinal chords together. The diagonal concrete compression struts, which discretely simulate the concrete compressive stress field, are connected to the ties and longitudinal chords at rigid nodes to complete the static equilibrium of the truss. Such truss model analogy demonstrated its convenience and potential in analyzing the strength of reinforced concrete members due to its visible nature to represent failure mechanism. Significant contributions have been made by many researchers to the development of truss models

*Corresponding author, Lecturer, E-mail: tctngoc@hcmiu.edu.vn

of reinforced concrete beams subjected to shear and flexure. However, the utilization of this method to capture the ultimate shear strength of non-seismically detailed columns which are vulnerable to shear failure is rather limited. The objective of this paper is to propose a strut-and-tie model which is able to predict the ultimate shear strength of non-seismically detailed columns.

The paper reported herein comprises two parts. The first part presents the modeling procedures for the seven full-scale shear-critical reinforced concrete columns which were tested by Lynn (2001) and Sezen (2002). The second part further examines the developed model through a comparison with the experimental results obtained from the test of a non-seismically detailed reinforced concrete column. The major focus of this paper is to demonstrate the capability of the strut-and-tie modeling approach in predicting the ultimate shear strength of non-seismically detailed reinforced concrete columns subjected to reverse cyclic loadings. Good correlations with the experimental data obtained reveal the great potential of implementing the strut-and-tie modeling approach in seismic analysis and design of reinforced concrete structures.

2. Previous design equations for ultimate shear strength of columns

2.1 ACI 318 (2008) code provisions

The ACI Building Code on shear strength suggests the following additive equation to express the shear strength of axially loaded members

$$V = V_c + V_s \tag{1}$$

Where

$$V_c = 0.166\sqrt{f_c'}\left(1 + \frac{P}{13.8A_g}\right)bd \text{ (MPa)} \tag{2}$$

The contribution of truss mechanism is taken as

$$V_s = \frac{A_v f_y d}{s} \tag{3}$$

Where A_v = the total transverse steel area within spacing s; f_y = yield strength of transverse steel; d = effective depth of the section.

2.2 Priestley et al.'s (1994) equation

Priestley *et al*. proposed an additive shear equation

$$V = V_c + V_s + V_a \tag{4}$$

Where

$$V_c = k\sqrt{f_c'}A_e \tag{5}$$

k depends on the displacement ductility factor μ_Δ, which reduces from 0.29 in MP units for $\mu_\Delta \le 2.0$ to 0.1 in MPa units for $\mu_\Delta \ge 4.0$; and is taken as 0.8. The shear strength contribution by truss mechanism is given by

$$V_s = \frac{A_v f_y h_c}{s}\cot\theta \tag{6}$$

Where h_c = the core dimension measured center-to-center of the peripheral transverse reinforcements; and θ = the angle of truss mechanism, taken as 30 degrees.

The shear strength enhancement by axial load is given by

$$V_a = P\tan\alpha = \frac{D-x}{2D(M/VD)}P \tag{7}$$

Where D = section depth; x = the compression zone depth, which can be determined from flexural analysis; and (M/VD) = shear aspect ratio.

2.3 Sezen and Moehle's (2004) equation

Sezen and Moehle (2004) developed a shear strength model, which applied for lightly transverse reinforced columns accounting for apparent strength degradation associated with flexural yielding. The empirical model is based on theoretical concepts of sectional shear resistance but is calibrated to test data. The shear strength based on Sezen and Moehle's model (2004) is defined as

$$V_n = V_s + V_c = k\frac{A_{st}f_{yt}d}{s} + k\left(\frac{0.5\sqrt{f'_c}}{a/d}\sqrt{1+\frac{P}{0.5\sqrt{f'_c}A_g}}\right)0.8A_g \text{ (MPa)} \tag{8}$$

Where V_s and V_c are shear contributions assigned to steel and concrete; k is a parameter equal to 1 for displacement ductility less than 2, equal to 0.7 for displacement ductility more than 6, and varies linearly for intermediate displacement ductility; A_{st} = area of shear reinforcement parallel to horizontal shear force within spacing s; f_{yt} = yield strength of transverse reinforcement; d = effective depth (= 0.8 h, where h = section depth parallel to shear force); P = axial compression force; A_g = gross section area; and a/d = shear span/effective depth.

3. Modeling procedures

For a given member and loading system, there are several possible truss models to represent the complex stress fields inside the member. The most ideal model is the one that closely matches the actual stress fields in the member. The model was developed based on visible crack patterns observed on the test specimens. The specimen is idealized as a series of concrete struts and steel ties interconnected at nodes to form a strut-and-tie model.

A typical graphical presentation of the overall configuration of the strut-and-tie model for Lynn (2001), Sezen's (2002) specimens (as shown in Table 1) based on the visible crack patterns observed on the test specimens is illustrated in Fig. 1. The inclined struts which follow the inclination of shear cracks observed from experiments consist of concrete. The longitudinal reinforcement steel bars, was clustered in the two vertical members, each of which thus contains half of the number of bars. The concrete contribution in the longitudinal tensile chords was ignored due to extensive flexural cracking in the flexural tension zone observed from experiments while the concrete in the flexural compression zone can be considered as part of the longitudinal compressive

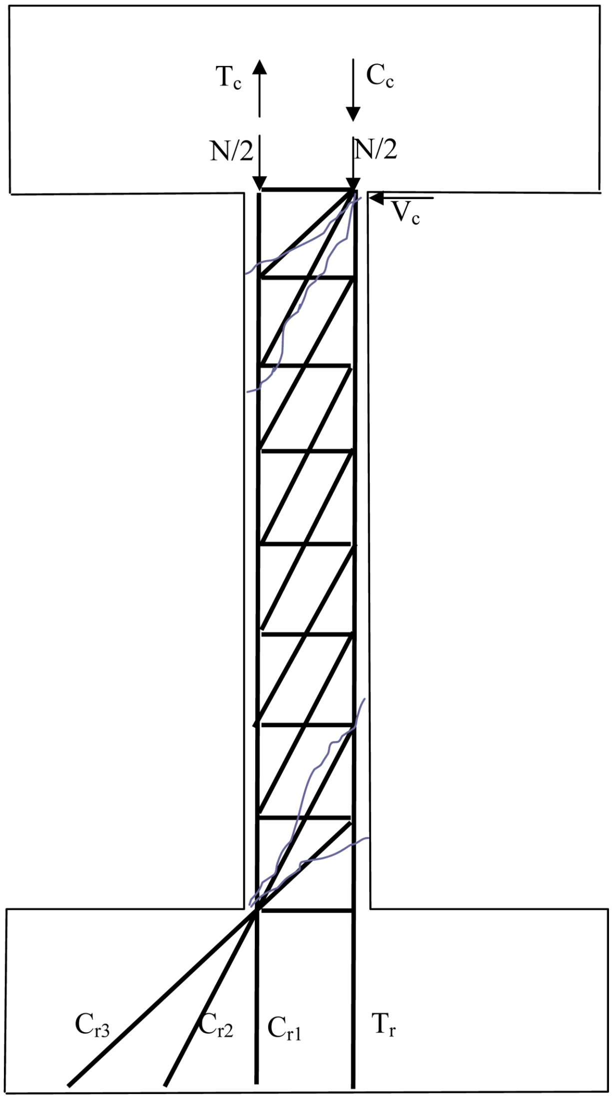

Fig. 1 Typical Strut-and-Tie Model for Lynn (2001), Sezen (2002)'s Specimens

chord. The depth of the truss model was defined as follows

$$jd = \frac{M_f}{A_s f_y} \tag{9}$$

Where M_f = theoretical flexural moment capacity of the column section, f_y is the yield strength of longitudinal reinforcement and A_s is the area of longitudinal reinforcing bars in the flexural tension zone. The vertical members of the truss are further connected to the transverse tension ties and diagonal compression struts of the truss model that represents the cracked concrete in compression. The compression struts and tension ties in the transverse direction are the primary mechanisms for shear transfer and resistance.

Collective ties concept was applied to the truss model. Their cross section is equal to the sum of all the adjacent ties substituted by the collective element. The concrete contribution is then integrated into the strut-and-tie model through a concept of equivalent transverse reinforcement. ACI 318 (2008) formula for concrete contribution was incorporated into the tie elements of the truss model to predict the ultimate shear capacity of the columns.

$$V_c = \left(0.16\sqrt{f_c'} + 17.2\rho_w\frac{V_u d}{M_u}\right)b_w d \le 0.3\sqrt{f_c'}\,b_w d \tag{10}$$

The solution of the truss model gives the forces of each constituent element from each of the applied external loading N, V and M. In this strut-and-tie model, the moment applied to the top of the column was substituted by a pair of axial force applied at the node as illustrated in Fig. 1. The magnitude of these axial forces was calculated as follows

$$C_c = T_c = \frac{M_n}{jd} \tag{11}$$

Where M_n = the applied moment at the top of the column, jd is the depth of the truss as defined above.

The applied external forces N, V, T_c and C_c from the column critical section are transferred to the base of the specimen through the above strut-and-tie mechanism. At the column and bottom base interface, the applied forces are further transferred to the fixed-end support through T_r, C_{1r}, C_{2r} and C_{3r} elements. The strength of T_r is provided by the anchorage and bond of the longitudinal reinforcement bars into the base of the specimen while the strengths of C_{1r}, C_{2r} and C_{3r} are from the compressive strength of the base of the specimen. It was assumed that the strength of these elements was much larger than the strength of the elements of the strut-and-tie model.

The column reaches its ultimate shear capacity when one of the elements of the strut-and-tie model reaches its maximum capacity. The strength of each element of the strut-and-tie model will be defined at the next part of this paper.

3.1 Strength of tensile chords

The concrete contribution in the longitudinal tensile chords was ignored due to extensive flexural cracking in the flexural tension zone observed from experiments. Therefore, the strength of the tensile chords was only contributed from the longitudinal reinforcement bars. In this study, the yield strength of reinforcement bar was adopted to calculate the maximum strength of the tensile chords of the strut-and-tie model.

3.2 Strength of compressive chords

The strength of longitudinal compressive chords was contributed from the two sources: the longitudinal reinforcement bars and the concrete in the flexural compression zone. It was assumed that the steel bars and the concrete in the compressive chords reached their maximum strength simultaneously. The maximum strength of the steel bars in the compressive chords was assumed as the yield strength of the steel bars while the strength of concrete was reduced by the tensile cracks perpendicular to it. This paper adopted $0.8f_c'$ for the effective strength of concrete following Schlaich's (1987, 1991) suggestions. The area of concrete in the compressive chord was calculated

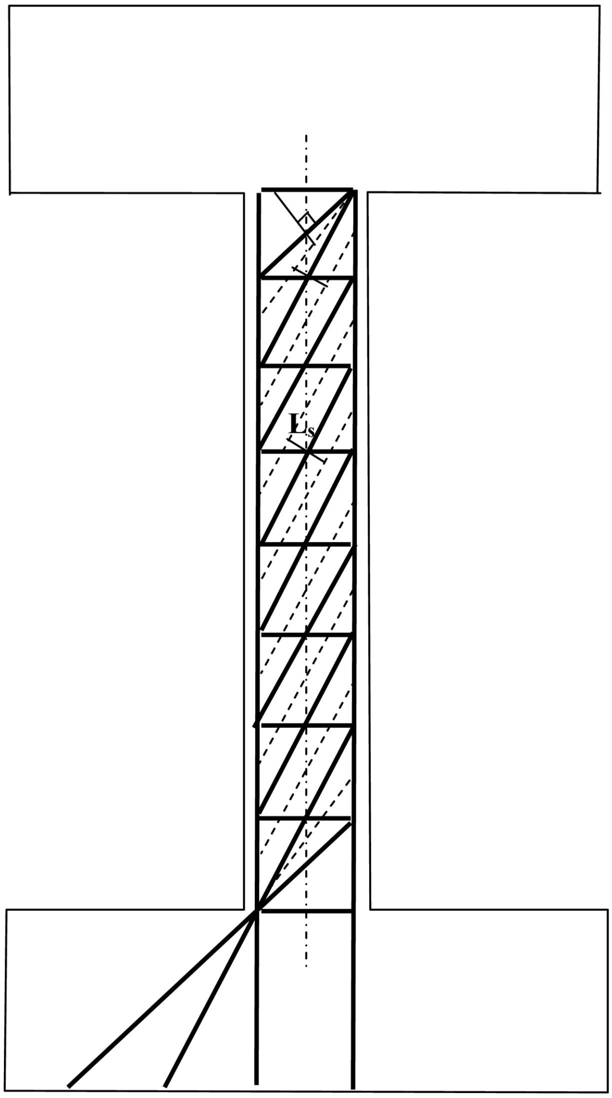

Fig. 2 Sizing of inclination struts

based on the bending theory at the ultimate strength of the column section.

3.3 Strength of struts

The diagonal compression struts are the discrete representation of the actual stress field inside the column. One strut covers the stress flow in its nearby region. As the stress flow is continuous in a column, the areas of the compression struts are determined from its geometrical consideration. An effective width, L_s is defined on this basis for each strut as shown in Fig. 2. The compressive strength of $0.4f_c'$ following Schlaich's (1987, 1991) suggestions was chosen for the diagonal compression struts to cater for skew cracks with extraordinary crack width.

Table 1 Database of non-seismically detailed columns

Specimen	Column Section							Transverse Reinforcement			Longitudinal Reinforcement		
	f_c' (MPa)	$\frac{P}{A_g f_c'}$	h (mm)	b (mm)	d (mm)	a (mm)	$\frac{a}{d}$	Diameter (mm)	Spacing (mm)	f_y (MPa)	No. of Bars	Diameter (mm)	f_y (Mpa)
Lynn (2001)													
3CLH18	25.6	0.09	457	457	393	1473	3.75	9.5	457	400	8	32.3	331
2CLH18	33.1	0.07	457	457	397	1473	3.71	9.5	457	400	8	25.4	331
2CMH18	25.7	0.28	457	457	397	1473	3.71	9.5	457	400	8	25.4	331
3CMH18	27.6	0.26	457	457	393	1473	3.75	9.5	457	400	8	32.3	331
3CMD12	27.6	0.26	457	457	393	1473	3.75	9.5	305	400	8	32.3	331
Sezen (2002)													
2CLD12	21.1	0.61	457	457	392	1473	3.75	9.5	305	476	8	28.7	438
2CHD12	21.1	0.15	457	457	392	1473	3.75	9.5	305	476	8	28.7	438
Current Experiment													
SC01	49.3	0.03	350	350	301	850	2.82	6.0	125	393	8	25.0	409

Table 2 Ultimate shear capacity of the non-seismically detailed columns predicted by the proposed strut-and-tie model

Specimen	V_u (kN)	V_{ACI} (kN)	$V_{\text{Priestley}}$ (kN)	V_{Sezen} (kN)	V_{STM} (kN)	$\frac{V_{ACI}}{V_u}$	$\frac{V_{\text{Priestley}}}{V_u}$	$\frac{V_{Sezen}}{V_u}$	$\frac{V_{STM}}{V_u}$	Recorded Failure Mode	Failure Mode Predicted by STM
Lynn (2001)											
3CLH18	271.0	225.4	383.6	206.4	316.1	0.832	1.415	0.762	1.166	Tensile Yielding of Longitudinal Reinforcement	Tensile chord
2CLH18	240.0	252.9	409.3	224.9	242.6	1.054	1.705	0.937	1.011	Tensile Yielding of Longitudinal Reinforcement	Tensile chord
2CMH18	316.0	282.1	458.7	273.5	325.5	0.893	1.452	0.866	1.030	Compressive Yielding of Longitudinal Reinforcement	Compressive chord
3CMH18	338.0	287.6	468.1	275.8	415.2	0.851	1.385	0.816	1.228	Significant Opening of Shear Cracks	Second Layer Tie
3CMD12	356.0	385.3	594.8	352.3	430.5	1.081	1.671	0.990	1.209	Tensile Yielding of Longitudinal Reinforcement	Tensile chord
Sezen (2002)											
2CLD12	315.0	317.0	496.9	285.0	346.1	1.006	1.577	0.905	1.099	Tensile Yielding of Longitudinal Reinforcement	Tensile chord
2CHD12	359.0	410.0	591.3	409.0	344.5	1.142	1.647	1.139	0.960	Compressive Yielding of Longitudinal Reinforcement	Compressive chord
Current Experiment											
SC01	357.1	310.5	530.9	309.5	358.2	0.869	1.486	0.868	1.003	Significant Opening of Shear Cracks	Second Layer Tie

3.4 Strength of ties

The strength of each tie of the model was defined as the summation of steel contribution obtained from strain gauge readings at the ultimate shear capacity state and the concrete contribution calculated from ACI 318 (2008) formula.

3.5 Analytical results

The ultimate shear capacity of Lynn (2001), Sezen's (2002) specimens, which were calculated by the proposed strut-and-tie model, are shown in Table 2. It was found that the mean value of V_{STM}/V_u was 1.082, showing a good correlation between the strut-and-tie model and the experimental data. The proposed strut-and-tie model was able to predict well not only the ultimate shear capacity but also the mode of failure of the specimens as illustrated in Table 2. The model predicted higher ultimate shear strength value comparing to experimental one was due to the incorporation of the concrete contribution into the model. The proposed strut-and-tie model could be used to give an upper bound for the ultimate shear capacity of the available experimental data.

4. Experimental studies

4.1 Specimen and test procedure

To further validate the proposed strut-and-tie model, a full-scale non-seismically detailed column, which is often found in existing structures in Singapore and other parts of the world were constructed and tested. Fig. 3 illustrates the schematic dimensions and detailing of the Specimen SC01. The specimen is shear-critical columns with a shear span to depth ratio of about 2.43. SC01 had a clear height of 1700 mm and a cross section of 350 mm × 350 mm. The section dimension can be considered as a 1/1 scale of a prototype column in a moment-resisting frame structure. The column with 8 T25 longitudinal bars has a longitudinal reinforcement ratio of 3.21%. The transverse bars were spaced at 125 mm at both ends and 200 mm at the center of the columns. Each set of transverse reinforcement was made of a peripheral hoop with 135 degrees hooks. The specimen was built with grade 40 concrete. The concrete compressive strength of the test unit obtained from the average of three $\phi 150\,\text{mm} \times 300\,\text{mm}$ concrete cylinders was 49.3 MPa. High deformed reinforcement bar T25 was used as main bars in the test units while mild steel bar R6 was used as transverse reinforcements. The yield strengths, f_y of the T25 and R6 bars used in the test were 409.3 MPa and 392.6 MPa while the ultimate strengths, f_u were 619.9 MPa and 579.7 MPa respectively.

A schematic of the loading apparatus is shown in Fig. 4. The specimen was subjected to quasi-static load reversals that simulated earthquake loadings. A reversible horizontal load was applied to the top of the columns using a double-acting 1000 kN capacity long-stroke dynamic actuator which was mounted on the reaction wall. The actuator was pinned at both ends to allow rotation during the test. The loading device was manually operated to achieve a better control on the load increment. The base of the column was fixed to a strong floor through four post-tensioned bolts. The axial load was applied to the column using two double-acting 1000 kN capacity dynamic actuators through a transfer beam.

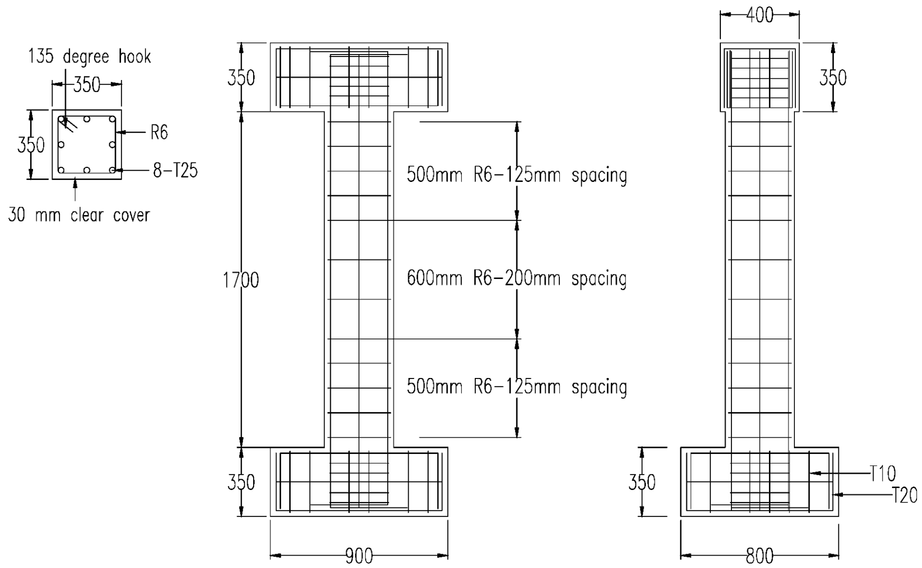

Fig. 3 Reinforcement details of test specimen

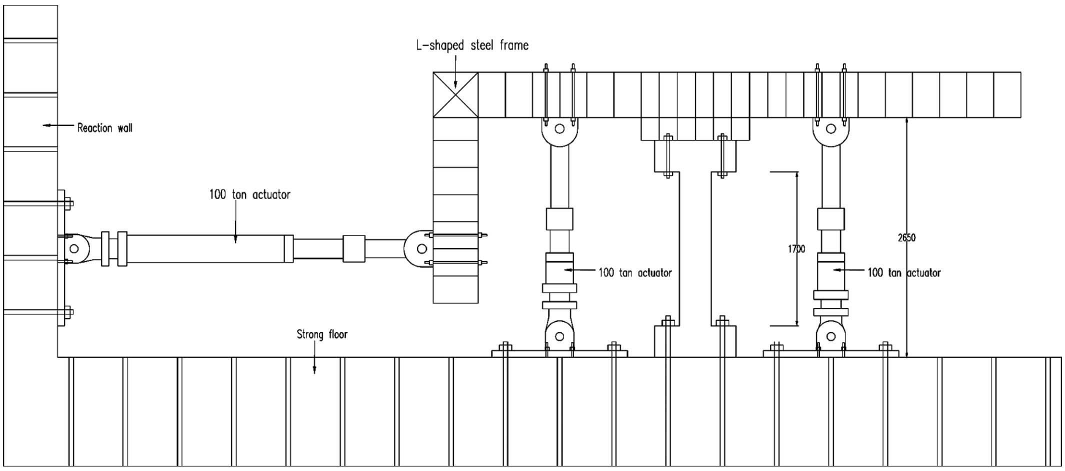

Fig. 4 Test setup

Before the start of each test, the column axial load was slowly applied to the column until the designated level of $0.3f_c'A_g$ was achieved. During each test, the column axial load was maintained manually by adjusting the actuators after each load step. The lateral load was applied cyclically through the dynamic actuator in a quasi-static fashion at the top end of the column as shown in Fig. 4. The loading procedure consisted of displacement-controlled steps (Lu 2012, Said 2009) beginning at a 1/2000 (0.05%) drift ratio followed by steps of 1/1000 (0.1%), 1/600 (0.17%), 1/400 (0.25%), 1/300 (0.33%), 1/200 (0.50%), 1/150 (0.67%), 1/100 (1.0%), 1/75 (1.33%) and 1/55 (1.82%) drift ratio. At the drift ratio 1/2000, each drift ratio step consisted of 1 cycle of push and

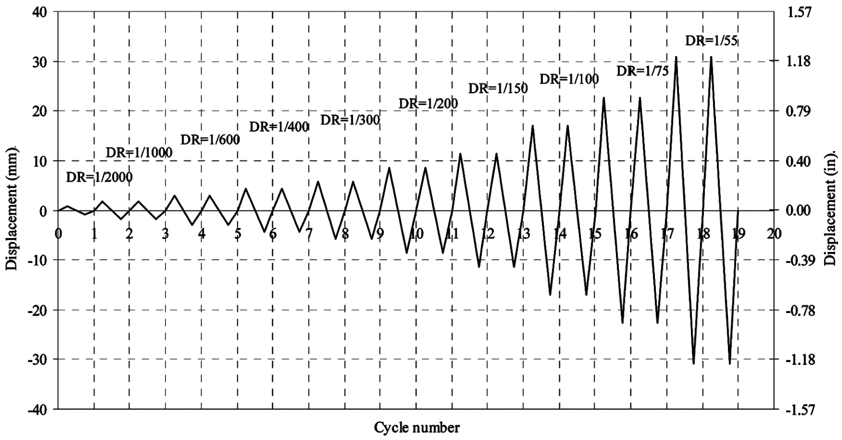

Fig. 5 Loading procedure

pull, after which 2 cycles of push and pull were applied. The typical loading procedure is illustrated in Fig. 5.

In order to obtain the test results that explained most of the observation qualitatively, instrumentations such as the dynamic actuator, strain gauges, LVDTs and displacement transducers were installed. The specimen was loaded horizontally using dynamic actuator where the load applied was recorded in the data acquisition system. The behavior of reinforcement bars was observed by installing strain gauges in the bars prior to casting of the specimens. LVDTs and displacement transducers were installed to observe the displacement behavior of the column at various locations during the test.

4.2 Experimental results and discussions

The general behaviors of the tested specimen were identified based on the load-displacement hysteresis responses (Fig. 6) and visible crack patterns (Fig. 7). All test results described herein are in correspondence with the imposed drift ratios, which were expressed in an abbreviated form. For example, ±DR of 1.0%, the positive and negative signs indicate the directions of the loading cycles while DR of 1.0% stands for a drift ratio of 1.0%.

Fig. 6 shows the load-displacement hysteresis loops of the specimen. The hysteresis loops show the degradation of stiffness and load-carrying capacity during repeated cycles due to the cracking of the concrete and yielding of the reinforcing steels while, the low attainment of stiffness and strength were attributed to the shear cracks along the specimens. Pinching was seen in the hysteresis loops of the specimen when a drift ratio of 1.0% was applied, leading to limited energy dissipated as shown in Fig. 6. The specimen reached its maximum horizontal strength in the first cycle at a drift ratio of 1.0%. At the next drift ratio of 1.33%, the peak lateral load attained was only 82.3% of the maximum recorded value of the specimen. Continuing cycling caused additional damage and loss of lateral resistance. During the first push cycle at a drift ratio of 2%, the column failed catastrophically due to the failure of the transverse reinforcements. At this state, the applied axial load dropped suddenly from 1804 kN to 400 kN showing the brittle behavior of the specimen with non-seismic detailing.

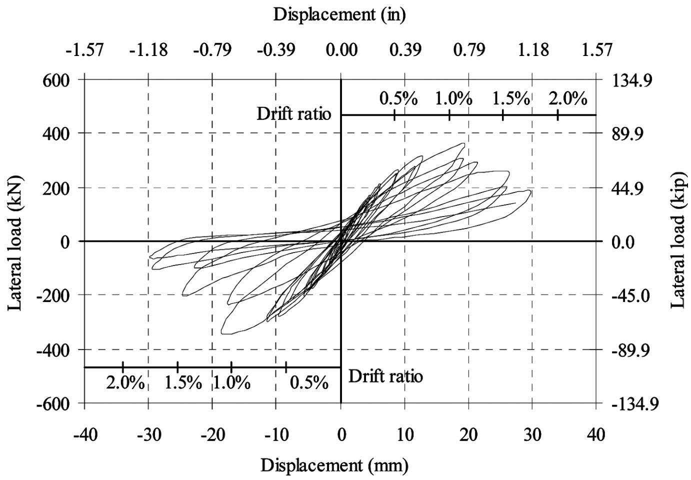

Fig. 6 Hysteresis loops of specimen SC01

4.3 Shear resisting mechanisms at the ultimate shear capacity

A strut-and-tie model, similar to that proposed in the previous part of this part, can be developed for investigating force transfer in the tested column at the ultimate shear capacity state as shown in Figs. 7 and 8. Good correlations with the experimental data have been obtained as shown in Table 2.

A graphical presentation of the overall configuration of this strut-and-tie model is illustrated in Fig. 8. Compressive members are shown as dotted lines while tensile members are shown as solid lines. The inclined struts consist of concrete that varies from 19 to 35 degrees, corresponding to the inclination of shear cracks observed from experiments. The longitudinal reinforcement, 8T25 mm bars, was clustered in the two vertical members, each of which thus contains 4 bars.

As shown in Fig. 8, the major tie T_1 is required to carry a tensile force of 182.8 kN. The steel contribution of T_1 of 19.2 kN was obtained from the strain gauge readings and measured properties of the steel link. Hence, the remaining amount of the tensile force of 163.6 kN will be carried by concrete. This is equal to the value obtained from ACI 318 (2008) for concrete contribution. As shown in Table 2, the predicted ultimate shear capacity based on the proposed strut-and-tie model was 358.2 kN. It was found that V_{STM}/V_u = 1.003, showing a good correlation between the strut-and-tie model and the experimental data. The proposed strut-and-tie model predicted higher ultimate shear strength value was due to the incorporation of the concrete contribution into the model. The proposed strut-and-tie model could be used to give an upper bound for the ultimate shear capacity of test specimen.

5. Limitations and recommendations

According to the findings of the present study, the usage of the proposed strut-and-tie model in the prediction of shear strength of non-seismically detailed columns can be improved in the following aspects. Firstly, the inclination of the diagonal struts is very much predefined when

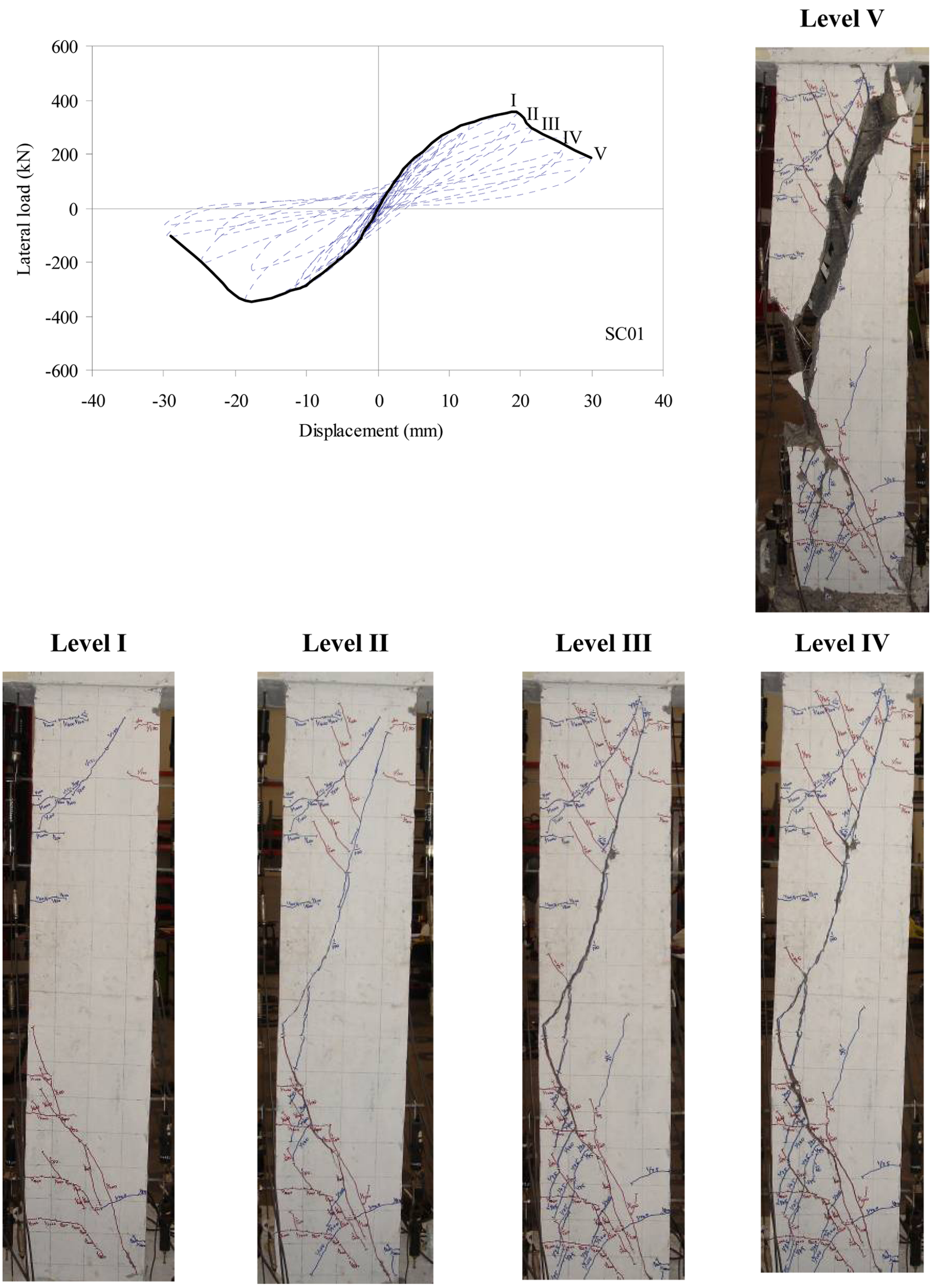

Fig. 7 Cracking patterns of tested specimen

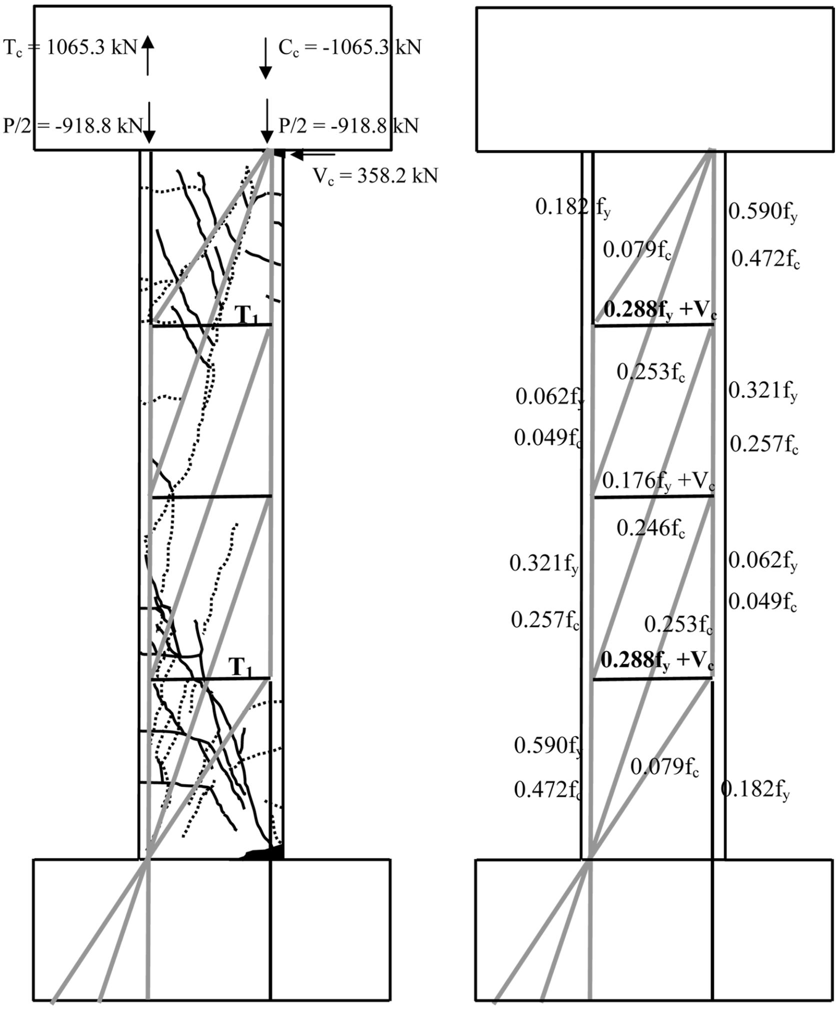

Fig. 8 Resisting mechanism at the ultimate shear capacity

forming the strut-and-tie model. A more rigorous procedure can be developed to overcome this limitation. Secondly, the proposed strut-and-tie model is an analytical tool to understanding the mechanisms of RC columns subjected to flexure and shear. Due to its indeterminate nature, it can only have limited usage in design. An approach with variable angle truss model enabling hand calculation for strength is needed. It is concluded that further researches should focus on these aspects to further improve the proposed truss model.

6. Conclusions

Based on the results of this study, the following conclusions can be drawn:

A full-scale non-seismically detailed reinforced concrete column, which is commonly found in existing structures in Singapore and other parts of the world, was tested under a constant axial load and quasi-static cyclic loadings simulating earthquake actions. The test specimen exhibited apparent shear and axial load failures. Gradual shear strength deterioration and low attainment of structural stiffness were observed after the specimens reached its maximum lateral load capacity. The low attainment of stiffness and strength were attributed to the shear cracks along the specimens. Test results showed that the responses of non-seismically detailed columns were brittle and a significant reduction of the lateral load capacity was observed when the drift ratio reached 1.33%. The experimental results also showed that under high axial loads, the non-seismically detailed columns could not maintain its axial loads well beyond a drift ratio of 2.0% and axial failure occurred at a drift ratio of 1.82% just after shear failure. Sliding along the diagonal shear cracks was observed prior to the axial failure.

The complicated resisting mechanism in the non-seismically detailed columns could be analyzed by a strut-and-tie model incorporating the concrete contribution. It is recommended that the analytical model proposed in this paper is useful to determine the ultimate shear capacity of the non-seismically detailed columns, which exhibit the shear failure behaviors.

The proposed strut-and-tie model provides a good estimation of the ultimate shear capacity of non-seismically detailed columns. However, due to its empirical natures (the inclination of the diagonal struts is very much predefined based on visible crack patterns observed on the test specimens) this strut-and-tie model has limited usage in design. The strut-and-tie model proposed herein is only an analytical tool to understand the shear resisting mechanism of non-seismically detailed columns subjected to reverse cyclic loadings.

References

ACI Committee 318 (2008), *Building Code Requirements for Structural Concrete (ACI 318-08) and Commentary*, American Concrete Institute, Farmington Hills, Mich.

Brown, M.D., Sankovichm, C.L., Bayrak, O.Z. and Jirsa, J.O. (2006), "Behavior and efficiency of bottle-shaped struts", *Struct. J.*, *ACI*, **103**(3), 348-354.

Khoo, J.H. and Li, B. (2007), "Modelling of reinforced concrete sub-frame sub-assemblage under cyclic load reversals", *J. Earthq. Eng.*, 215-230.

Kiousis, P.D., Papadopoulos, P.G. and Xenidis, H. (2010), "Truss modeling of concrete columns in compression", *J. Eng. Mech., ASCE*, **136**(8), 1006-1014.

Lu, X.L., Urukap, T.H., Li, S. and Lin, F.S. (2012), "Seismic behavior of interior RC beam-column joints with additional bars under cyclic", *Earthq. Struct*., **3**(1), 37-57.

Lynn, A.C. (2001) "Seismic evaluation of existing reinforced concrete building columns", PhD Thesis, Department of Civil and Environmental Engineering, University of California, Berkeley, Calif.

Priestley, M.J.N., Verma, R. and Xiao, Y. (1994), "Seismic shear strength of reinforced concrete columns", *J. Struct. Eng.*, *ASCE*, **120**(7), 2310-2329.

Said, A.M. (2009), "Damage characterization of beam-column joints reinforced with GFRP under Reversed Cyclic Loading", *Smart Struct. Syst.,* **5**(4), 448-455.

Schlaich, J. and Schafer, K. (1991), "Designs and detailing of structural concrete using strut-and-tie models", *The Struct. Eng.*, **69**(6), 113-125.

Schlaich, J., Schafer, K. and Jennewein, M. (1987), "Toward a consistent design of structural concrete", *PCI J.*, **32**(3), 74-150.

Sezen, H. (2002), "Seismic response and modeling of reinforced concrete building columns", PhD Thesis, Department of Civil and Environmental Engineering, University of California, Berkeley, Calif.

Sezen, H. and Moehle, J. (2004), "Shear strength model for lightly reinforced concrete columns", *J. Struct. Eng.*, *ASCE*, **130**(11), 1692-1703.

Yang, K.H. and Ashour, A.F. (2011), “Strut-and-tie model based on crack band theory for deep beams”, *J. Struct. Eng. ASCE*, **137**(10), 1030-1038.

Zhang, N. and Tan, K.H. (2007), “Direct strut-and-tie model for single span and continuous deep beams”, *Eng. Struct.*, **29**(11), 2987-3001.